Globally Linearizing Control for a Magnetic Microrobot Navigating Within a Blood Vessel

NACERA ICHEDDADENE[1], MEZIANE LARBI[2], AHMED MAIDI[1], KARIM BELHARET[2]
[1]L2CSP Laboratory, Mouloud MAMMERI University, 15 000 Tizi-Ouzou, ALGERIA
[2]HEI Campus Centre, PRISME EA 4229, Chateauroux, FRANCE.

Abstract: - In this paper, the globally linearizing control scheme is employed to guide an endovascular magnetic microrobot navigating within a blood vessel with the objective of reaching a desired target following a trajectory generated via a joystick device. First, we derive the 1D nonlinear dynamical model for the magnetic microrobot. Subsequently, a stabilizing state feedback is designed based on the relative degree from geometric control, resulting in a closed-loop linear system. To ensure the tracking of a time-varying trajectory and reject disturbances, an external proportional-integral controller with a bias is used to define the external variable of the resulting linear system. The performance of the GLC is evaluated via numerical simulations. The obtained results demonstrate the output tracking and disturbance rejection capabilities of the GLC scheme.

Key-Words: - Magnetic microrobot, geometric control, relative order, globally linearizing control, output tracking.

Received: July 15, 2023. Revised: July 13, 2024. Accepted: August 12, 2024. Published: September 27, 2024.

1 Introduction

Due to their small size, wireless control, and power capabilities, microrobots have successfully been applied in biomedical settings to perform tasks with reduced invasiveness, [1]. Among these applications, one can cite targeted drug delivery, brachytherapy, tissue reconstruction, diagnosis and hyperthermia, to name a few, [2], [3], [4].

To achieve these tasks with high accuracy, particularly in complex environments, control techniques play a key role. Indeed, to successfully reach the target in environments with bifurcations and to access the most critical confined areas requiring treatment, precise trajectory tracking is crucial. Thus, numerous open-loop and closed-loop control strategies have been developed in the literature; a comprehensive review can be found in [2], [5], [6]. Nevertheless, due to nonlinearities, internal and external disturbances, uncertainties, and noise, the performance of open-loop control is limited and may become unstable, [2]. Therefore, to achieve precise motion despite disturbances and uncertainties, the use of closed-loop control techniques is required.

Model-based techniques have been extensively studied in the literature, using either a linear or a nonlinear model of the microrobot. When blood velocity is assumed to be zero, a linear model can be used. In this case, several well-established control strategies have been employed. These include the use of a PID controller, [7], a model predictive controller (MPC), [8], a tolerant ISS-based control approach, [9], robust control, [10], observer-based control, [11], and sliding mode control, [12].

Actually, since blood velocity is variable, a nonlinear model is required to capture the dynamic behavior of the microrobot. However, designing easy-to-implement controls using a nonlinear model that achieve precise tracking trajectories despite disturbances and uncertainties is a complex task. Few approaches have been explored in the literature, including backstepping control, [13], [14], and observer-based control, [15], [16]. This observation motivates the application of alternative techniques to improve microrobot control performance in dynamic environments.

Globally linearizing control (GLC), [17], [18], [19], is an interesting alternative control approach for nonlinear systems with a relative degree equal to its order, which applies to the microrobot. In this case, a stabilizing state feedback can be designed within the framework of geometric control, resulting in a closed-loop linear system. Then, to address disturbances and uncertainties, an external controller is used to define the external input of the resulting linear system, [17], [19]. Many successful applications of GLC for highly nonlinear systems have been reported in the literature, [18], [19], [20], [21], [22].

In this work, the GLC is applied to solve the output tracking of a microrobot navigating within a blood vessel. The control objective is to steer the microrobot from its initial position to the desired target position following a time-varying trajectory generated by an operator via a joystick, despite environmental disturbances. The control design is achieved using a nonlinear model. A modified GLC that combines an external controller and a reference differentiator is adopted to achieve precise trajectory tracking. This study introduces the application of a modified GLC, marking a first in the field. By utilizing GLC with a nonlinear model, our work advances nonlinear control strategies for microrobots, demonstrating not only the efficacy but also the significant potential of GLC in enhancing microrobot navigation.

The manuscript is outlined as follows: Section 2 focuses on the modeling of the microrobot, presenting a comprehensive 1D nonlinear dynamic model that captures its behavior within a blood vessel environment. In Section 3, the paper delves into the design of the GLC for the microrobot, aiming to achieve precise and robust trajectory tracking despite environmental disturbances. Section 4 presents the simulation results, showcasing the effectiveness and performance of the GLC approach in terms of trajectory tracking accuracy and robustness against disturbances. Finally, Section 5 concludes the paper.

2 Microrobot modeling

Consider a spherical magnetic microrobot of mass m and a radius R that navigates within a cylindrical blood vessel along the $\vec{i}$-axis (Figure 1). In this section, a one-dimensional (1D) state-space model describing the behavior of the microrobot is presented. Thus, the position and velocity along the $\vec{i}$-axis are denoted by p_r and v_r, respectively. It is assumed that the microrobot is affected by the drag force F_d and the magnetic force F_m. The magnetic force F_m is used to move the microrobot by manipulating the magnetic field gradient B, [23].

2.1 Magnetic and drag forces

2.1.1 Magnetic force F_m

The microrobot is propelled through the blood vessels by the magnetic force F_m, induced by the magnetic coils of the electromagnetic actuation system (EMA) by manipulating the magnetic field gradient. The F_m force is defined by [11]:

$$F_m = \frac{m}{\rho_r} M \nabla B \tag{1}$$

where M and ρ_r represent the magnetization and the density of the microrobot, respectively. The ∇ denotes the gradient operator, and B stands for the magnetic field; hence, ∇B is the magnetic field gradient, which is used as the control variable.

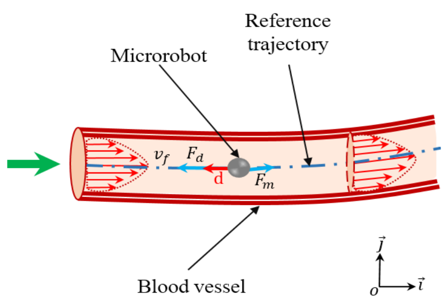

Figure 1: Forces acting on a microrobot navigating through a blood vessel.

2.1.2 Drag force F_d

The microrobot moving in a static or fluid environment experiences a hydrodynamic drag force F_d that opposes its displacement. The drag force F_d acting on a spherical microrobot with a frontal area A_f is given by [13]:

$$F_d = -\frac{1}{2}\rho_f (v_r - v_f)^2 A_f D_c \frac{v_r - v_f}{\|v_r - v_f\|} \tag{2}$$

where ρ_f and v_f are the density and velocity of the fluid, respectively, and D_c represents the drag coefficient.

Assuming that the microrobot navigates in a dynamic fluid, in this case the drag coefficient D_c is defined as [24]:

$$D_c = \frac{24}{R_e} + \frac{6}{1+\sqrt{R_e}} + 0.4 \tag{3}$$

where the Reynolds number R_e that determines the flow regime of the fluid is given by [13]:

$$R_e = \frac{2\rho_f (v_r - v_f) R}{\eta} \tag{4}$$

where η is the fluid viscosity.

Combining Equations (2), (3) and (4), it follows that

$$F_d = -6\pi R \eta (v_r - v_f) + \rho_f \pi R^2 (v_r - v_f)^2 \times \left(0.2 + \frac{3}{1+\sqrt{\frac{2\rho_f (v_r - v_f) R}{\eta}}} \right) \tag{5}$$

2.2 Microrobot model

Using Newton's fundamental law of dynamics leads to the ordinary differential equation, which describes the dynamic behavior of the microrobot and is given by:

$$m \dot{v}_r = F_m + F_d \tag{6}$$

Substituting F_m and F_d with their expressions from Equations (1) and (5), Equation (5) reduces to

$$\dot{v}_r = \alpha_1 (v_r - v_f) + \alpha_2 (v_r - v_f)^2 + \alpha_3 \frac{(v_r - v_f)^2}{1+\alpha_4\sqrt{(v_r - v_f)}} + \alpha_5 \nabla B \tag{7}$$

with

$$\alpha_1 = -\frac{9\eta}{2R^2\rho_r},\ \alpha_2 = -\frac{0.15\rho_f}{R\rho_r},\ \alpha_3 = -\frac{2.25\rho_f}{R\rho_r}$$

$$\alpha_4 = \sqrt{\frac{2\,R\,\rho_f}{\eta}},\ \alpha_5 = \frac{M}{\rho_r}$$

Defining the control variable $u = \nabla B$ and the state variables as the position and the velocity of the microrobot, i.e., $x_1 = p_r$ and $x_2 = v_r$ ($v_r = \dot{p}_r$), the state-space model of the microrobot obtained from Equation (7) is

$$\dot{x}(t) = f(x(t)) + g(x(t))\,u(t) \tag{8}$$
$$y(t) = h(x(t)) \tag{9}$$

where t is the time variable, $x = [x_1\ x_2]^T$ is the state vector, and the vector functions f, g, and h are defined as follows:

$$f(x(t)) = \left(\begin{array}{c} x_2(t) \\ \alpha_1\,w(t) + w^2(t)\left(\alpha_2 + \dfrac{\alpha_3}{1+\alpha_4\sqrt{w(t)}}\right) \end{array}\right) \tag{10}$$

$$g(x(t)) = \left(\begin{array}{c} 0 \\ \alpha_5 \end{array}\right) \tag{11}$$

$$h(x(t)) = x_1(t) \tag{12}$$

with $w(t) = x_2(t) - v_f$.

3 Globally linearizing control design

The objective consists in designing a control law u (magnetic field gradient) that moves the microrobot from a known initial position y_i to a desired target y_f in the blood vessel following a time-variable desired trajectory y^d. For this purpose, it is proposed to use the GLC strategy, [17], [18], [19], to solve this output tracking problem.

The GLC scheme consists of two control loops, [18]. The inner loop uses state feedback that yields in the closed loop a linear system $v - y$. Then, for robustness and disturbance rejection purposes, an outer loop is used to define the external variable v by means of the external controller.

The GLC design involves the following two steps, [17], [18], [19]:

1. Design of the linearizing state feedback in the framework of geometric control,
2. Design of the external control using the resulting linear system $v - y$.

3.1 Design of the state feedback

The design of the state feedback is carried out in the frame work of geometric control based on the concept of the relative degree, [25], [26]. The relative order σ refers to the minimum number of times that the output y needs to be differentiated to directly relate it to the input u. Thus, using the Lie derivative, [19], [25], [26], the time derivatives of the output y can be expressed as follows:

$$\begin{aligned}\dot{y}(t) &= L_f h(x) \\ &= x_2(t)\end{aligned} \tag{13}$$
$$\begin{aligned}\ddot{y}(t) &= L_f^2 h(x) + L_g L_f h(x)\,u(t) \\ &= \alpha_1\,w(t) + w^2(t)\,\varphi(w(t)) + \alpha_5\,u(t)\end{aligned} \tag{14}$$

with

$$\varphi(w(t)) = \alpha_2 + \alpha_3\,\frac{1}{1+\alpha_4\sqrt{w(t)}} \tag{15}$$

From (14), it can be seen that the control u appears linearly in the second time derivative of the output y, that is, $L_g L_f h(x) \neq 0$, hence the relative degree $\sigma = 2$. As σ is the same as the order $n = 2$ of the microrobot, the microrobot can be fully linearized, and the GLC can be successfully applied. Consequently, an output stabilizing state feedback can be designed that achieves in closed loop the stable linear system $v - y$ given by

$$\tau_2\,\ddot{y}(t) + \tau_1\,\dot{y}(t) + y(t) = v(t) \tag{16}$$

where v is an external input, and τ_1 and τ_2 are tuning parameters. Therefore, using Equations (13) and (14), the linear system (16) reduces to

$$\tau_2\ \left(\alpha_1\,w + w^2\,\varphi(w)\right) + \tau_2\,\alpha_5\,u + \tau_1\,x_2 + y = v \tag{17}$$

Then, solving Equation (17) with respect to the control u yields the following output stabilizing state feedback.

$$\begin{aligned}u(t) = \frac{1}{\tau_2\,\alpha_5}\Big[&v(t) - y(t) - \tau_1\,x_2(t) - \tau_2\ (\alpha_1\,w(t) \\ &+ w^2(t)\,\varphi(w(t)))\Big]\end{aligned} \tag{18}$$

3.2 Design of the external controller

The state feedback (18) is designed by assuming that there are no disturbances. Consequently, this control law will be incapable of rejecting the disturbance. To overcome this problem, the external input $v(t)$ must be defined by an external controller.

Assumption 1 *The desired trajectory $y^d(t)$ is a known twice differentiable function, i.e., $y^d(t) \in \mathcal{C}^2$ ($\mathcal{C}$ being the space of twice differentiable functions).*

To achieve disturbance rejection and robustness against modeling errors, the solution consists of defining the external variable v by means of an external controller of the general form [18]

$$v(t) = b(t) + \int_0^t c(t-\tau)\,\left(y^d(\tau) - y(\tau)\right)\,d\tau \quad (19)$$

where c is the inverse of a given transfer function, and $b(t)$ is the external controller bias given by

$$b(t) = \mathcal{D}\,y^d(t) \quad (20)$$

where $\mathcal{D}$ is the differential operator defined as follows:

$$\mathcal{D}(.) = \tau_2\,\frac{d^2(.)}{dt^2} + \tau_1\,\frac{d(.)}{dt} + (.) \quad (21)$$

In this work, a PI controller is used to define the external variable, i.e.,

$$v(t) = \mathcal{D}y^d(t) + K_c\,e(t) + \frac{1}{T_i}\int_0^t e(\xi)\,d\xi \quad (22)$$

where K_c and T_i are the tuning parameters of the PI controller, and $e(t) = y^d(t) - y(t)$ is the tracking error. The GLC scheme is depicted in Figure 2.

Remark 1 *For a constant set-point $y^d(t)$, the external controller bias $b(t) = y^d(t)$ since $d^2y^d(t)/dt^2 = dy^d(t)/dt = 0$, i.e., $\mathcal{D} = 1$.*

For the tuning of the PI controller, the internal model control-based tuning method is used, [27]. The transfer function of the linear closed loop system (16) is given by

$$G(s) = \frac{Y(s)}{V(s)} = \frac{1}{\tau_2\,s^2 + \tau_1\,s + 1} \quad (23)$$

where Y and V are the Laplace transforms of y and v, respectively, and s is the Laplace variable. Thus, by choosing the tuning parameters τ_1 and τ_2 as follows:

$$\tau_1 = \gamma_1 + \gamma_2 \quad (24)$$
$$\tau_2 = \gamma_1\,\gamma_2 \quad (25)$$

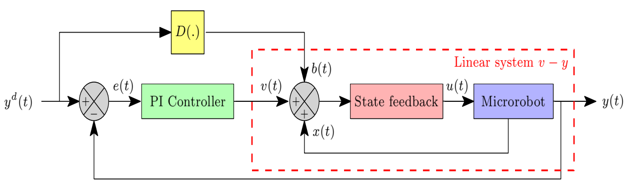

Figure 2: GLC scheme for the microrobot.

The transfer function (23) takes the following form:

$$\frac{Y(s)}{V(s)} = \frac{1}{(\gamma_1\,s + 1)\,(\gamma_2\,s + 1)} \quad (26)$$

and using the IMC-based tuning method yields the following PI controller tuning parameters, [27]

$$K_c = \frac{\gamma_1 + \gamma_2}{\tau} \quad (27)$$
$$T_i = \gamma_1\,\gamma_2 \quad (28)$$

where τ is the desired closed loop time constant.

4 Numerical simulation

In this section, the output tracking performance of the GLC is assessed through numerical simulation. Table 1 and Table 2 provide the microrobot parameters and the tuning parameter of GLC, respectively. It is assumed that the velocity of the blood v_f is time-varying, indicating an internal disturbance. The expression of v_f is [13]:

$$v_f(t) = 0.035\,(1 + 1.15\,\sin(2\,\pi\,t)) \quad (29)$$

Table 1: Microrobot parameters, [15].

Parameter	Value
Microrobot radius	$R = 250 \times 10^{-6}$ [m]
Fluid density	$\rho_f = 1060$ [Kg/m^3]
Fluid viscosity	$\eta = 16 \times 10^{-3}$ [Pa.s]
Microrobot density	$\rho_r = 7500$ [Kg/m^3]
Microrobot Magnetization	$M = 1.23 \times 10^6$ [A/m]

Table 2: GLC tuning parameters.

State feedback	PI controller
$\gamma_1 = 0.7692$ s	$K_c = 3.01$
$\gamma_2 = 5.2631$ s	$T_i = 6.03$ s

Evaluations of the performance of the GLC are conducted both with and without disturbance.

The desired reference y^d is generated by an operator using a joystick. The whole control scheme is summarized by Figure 3.

4.1 Results

For the first simulation run, the control objective consists of moving the microrobot from its initial position to a desired target following the generated trajectory y^d while the disturbance v_f is maintained constant. The obtained results are given by Figure 4. In the second simulation run, the microrobot is tasked

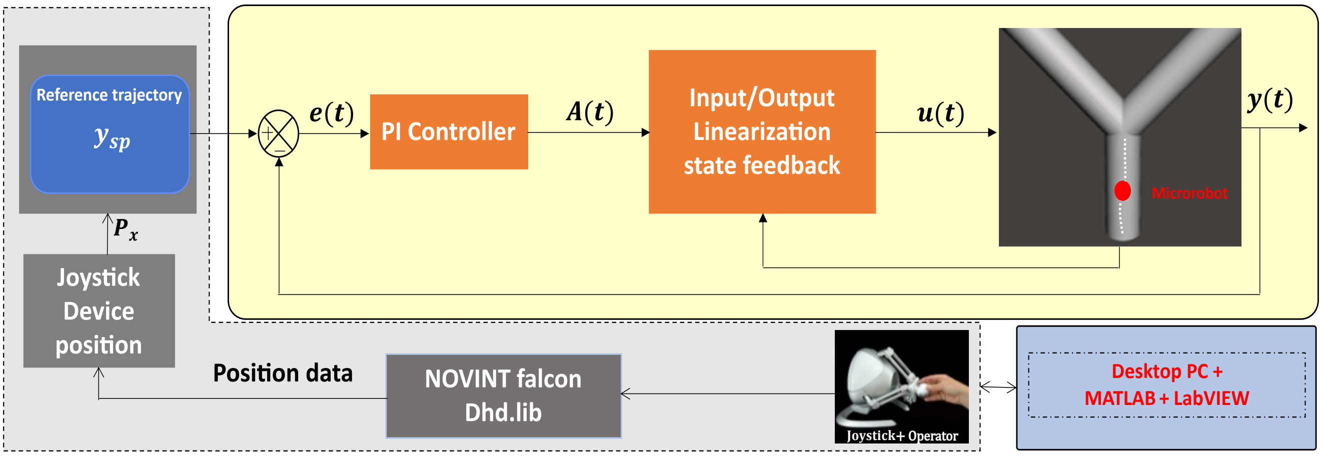

Figure 3: GLC scheme based on a joystick for a microrobot.

with reaching the desired target following the trajectory provided by the joystick, even with the sudden variation of the fluid velocity. To evaluate the performance in this situation, the following variation is assumed for the blood velocity:

$$v_f(t) = \begin{cases} 0.035\,(1 + 1.15\,\sin(2\,\pi\,t)) & t < 12\,s \\ \dfrac{v_f(t)}{2} & t \geq 12\,s \end{cases} \tag{30}$$

Figure 5 gives the obtained results.

4.2 Discussion

From Figure 4, it can be observed that despite the time-varying internal disturbance v_f, the GLC scheme allows the microrobot to reach the desired target following the trajectory generated by the joystick. This good tracking is supported by the position tracking error given in Figure 4-c. Additionally, Figure 4-d clearly shows reasonable moves of the magnetic field gradient, i.e., the control variable does not exceed the authorized value of 10^{-2} T/m.

From Figure 5, it can be seen that the GLC successfully rejects the disturbance and forces the microrobot to regain its imposed trajectory. This result is corroborated by the evolution of the position tracking error (Fig. 5-c). Additionally, the magnetic field gradient remains within physically acceptable limits (Fig. 5-d).

The simulation results clearly demonstrate the effectiveness of the GLC in achieving precise output tracking for the microrobot, both in the absence and presence of disturbances.

5 Conclusion

In the present work, the GLC scheme is adopted to guide a microrobot navigating in a blood vessel to reach a desired target following a trajectory generated by an operator via a joystick. First, the 1D nonlinear dynamical model of the magnetic microrobot is derived using Newton's fundamental law of dynamics. Then, as the relative degree is equal to the order of the microrobot, a stabilizing state feedback is designed within the framework of geometric control. This state feedback yields a linear system in a closed loop. Hence, for robustness and disturbance rejection, the external variable involved in the state feedback is defined by an external PI controller. To address the tracking problem even in the case of a time-varying desired trajectory, the external variable is adjusted by adding a bias that represents the differentiation of the desired trajectory.

The output tracking and disturbance rejection performance of the GLC are evaluated through numerical simulation. The obtained results demonstrate the effectiveness of the GLC in achieving precise trajectory tracking for the microrobot.

Based on the findings of this study, we recommend extending the GLC method to more complex nonlinear models in 2D and 3D environments, developing an observer to estimate the microrobot velocity for practical implementation, and conducting real-world testing to validate the simulation results.

References:

[1] J. J. Abbott, K. E. Peyer, M. C. Lagomarsino, L. Zhang, L. Dong, I. K. Kaliakatsos, and B. J. Nelson, "How should microrobots swim?" *The International Journal of Robotics Research*, vol. 28, no. 11-12, pp. 1434–1447, 2009.

[2] T. Xu, J. Yu, X. Yan, H. Choi, and L. Zhang, "Magnetic actuation based motion control for microrobots: An overview," *Micromachines*, vol. 6, no. 9, pp. 1346–1364, 2015.

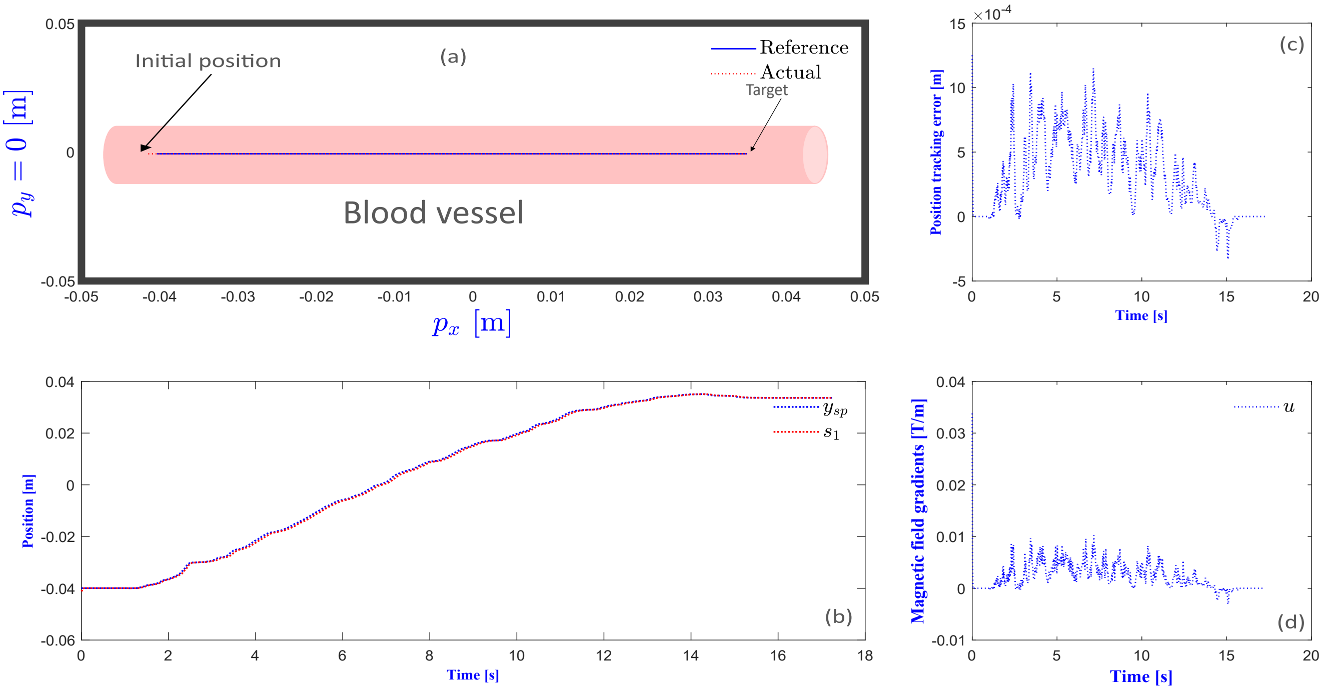

Figure 4: Output tracking without disturbance: (a) Actual and desired trajectories in the xy-plane. (b) Time evolution of the actual and desired trajectories. (c) Position tracking error. (d) Magnetic field gradients.

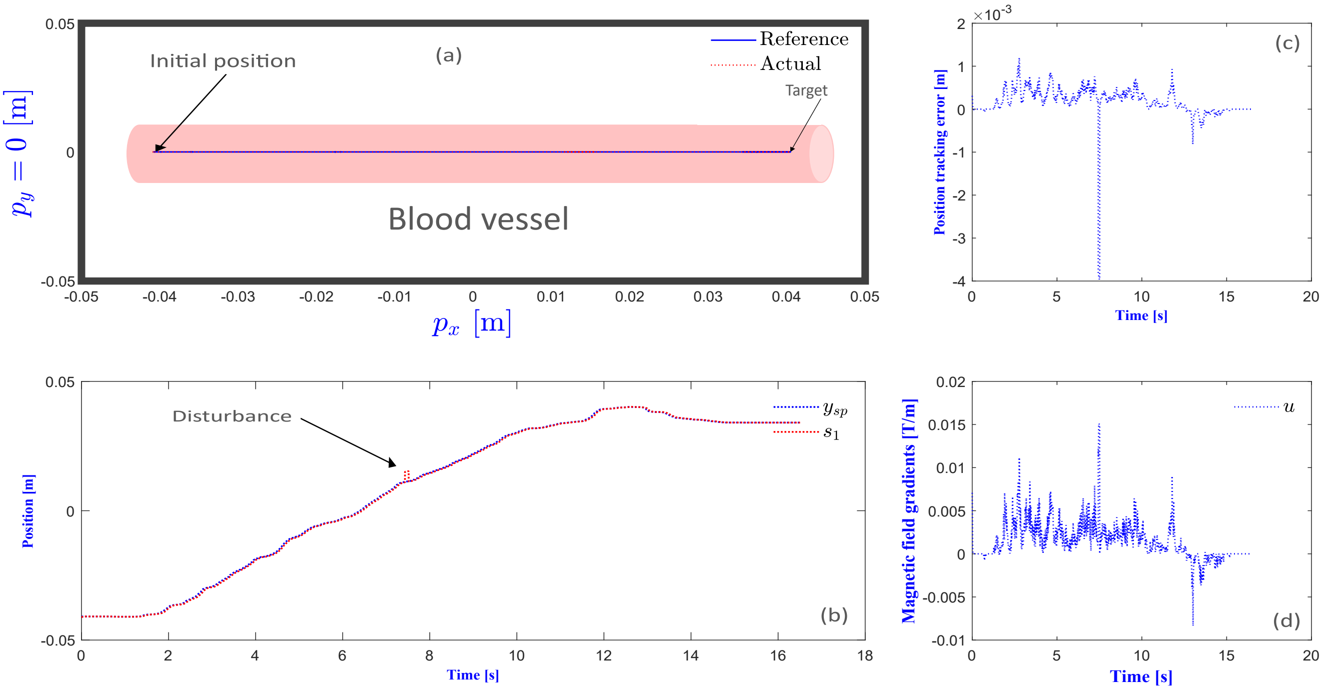

Figure 5: Output tracking in the presence of the disturbance: (a) actual and desired trajectories in the xy-plane. (b) Time evolutions of the actual and desired trajectories. (c) Position tracking error. (d) Magnetic field gradients.

[3] B. J. Nelson, I. K. Kaliakatsos, and J. J. Abbott, "Micro-robots for minimally invasive medicine," *Annual Review of Biomedical Engineering*, vol. 12, pp. 55–85, 2010.

[4] A. J. Moshayedi, A. S. Khan, M. Davari, T. Mokhtari, and M. Emadi Andani. Micro robot as the feature of robotic in healthcare approach from design to application: the State of art and

challenges. *EAI Endorsed Trans AI Robotics*, vol. 3, 2024.

[5] Y. Li, Y. Huo, X. Chu, and L. Yang, "Automated Magnetic Microrobot Control: From Mathematical Modeling to Machine Learning," *Mathematics*, vol. 12, no. 14, 2180, 2024.

[6] J. Jiang, Z. Yang, A. Ferreira, and L. Zhang. Control and autonomy of microrobots: recent progress and perspective. *Advanced Intelligent Systems*, vol. 4, no. 5, 2100279, 2022.

[7] S. Tamaz, R. Gourdeau, A. Chanu, J.-B. Mathieu, and S. Martel, "Real-time MRI-based control of a ferromagnetic core for endovascular navigation," *IEEE Transactions on Biomedical Engineering*, vol. 55, no. 7, pp. 1854–1863, 2008.

[8] K. Belharet, D. Folio, and A. Ferreira, "3D MRI-based predictive control of a ferromagnetic microrobot navigating in blood vessels," in *2010 3rd IEEE RAS & EMBS International Conference on Biomedical Robotics and Biomechatronics*, 2010, pp. 808–813.

[9] W. Ma, M. Xu, Z. Zhong, X. Li, and Z. Huan, "Closed-loop control for trajectory tracking of a microparticle based on input-to-state stability through an electromagnetic manipulation system," *IEEE Access*, vol. 8, pp. 46 537–46 545, 2020.

[10] J. Lu, Y. Liu, W. Huang, K. Bi, Y. Zhu, and Q. Fan, "Robust control strategy of gradient magnetic drive for microrobots based on extended state observer," *Cyborg and Bionic Systems*, vol. 2022, 2022.

[11] M. Larbi, E. Guechi, A. Maidi, and K. Belharet, "Observer-based control of a microrobot navigating within a 3D blood vessel along a trajectory delivered by a joystick device," *Machines*, vol. 11, no. 738, 2023.

[12] K. Meng, Y. Jia, H. Yang, F. Niu, Y. Wang, and D. Sun, "Motion planning and robust control for the endovascular navigation of a microrobot," *IEEE Transactions on Industrial Informatics*, vol. 16, no. 7, pp. 4557–4566, 2020.

[13] L. Arcese, M. Fruchard, and A. Ferreira, "Nonlinear modeling and robust controller-observer for a magnetic microrobot in a fluidic environment using MRI gradients," in *2009 IEEE/RSJ International Conference on Intelligent Robots and Systems*, 2009, pp. 534–539.

[14] M. Fruchard. Controllability and control synthesis of underactuated magnetic microrobots. *Automatica*, vol. 149, 110823, 2023.

[15] L. Sadelli, M. Fruchard, and A. Ferreira, "2D observer-based control of a vascular microrobot," *IEEE Transactions on Automatic Control*, vol. 62, no. 5, pp. 2194–2206, 2016.

[16] Q. Fan, H. Wang, X. Wu, and Y. Liu, "Magnetic microrobot control based on a designed nonlinear disturbance observer," in *2023 International Conference on Advanced Robotics and Mechatronics (ICARM)*, 2023, pp. 606–611.

[17] C. Kravaris and J. C. Kantor, "Geometric methods for nonlinear process control. 2. controller synthesis," *Industrial & Engineering Chemistry Research*, vol. 29, no. 12, pp. 2310–2323, 1990.

[18] M. Soroush and C. Kravaris, "Nonlinear control of batch polymerization reactor: an experimental study." *AIChE Journal*, vol. 38, no. 9, pp. 1429–1448, 1992.

[19] J. P. Corriou, *Process control - Theory and applications*. London: Springer, 2018.

[20] C. Kravaris and C. B. Chung, "Nonlinear state feedback synthesis by global input/output linearization," *AIChE Journal*, vol. 33, no. 4, pp. 592–603, 1987.

[21] J. Madar, J. Abonyi, and F. Szeifert, "Feedback linearizing control using hybrid neural networks identified by sensitivity approach," *Engineering Applications of Artificial Intelligence*, vol. 18, no. 3, pp. 343–351, 2005.

[22] M. Rafizadeh, A. Afshar, and H. Gharghi, "A GLC controller for the control of the methyl methacrylate polymerization," *IFAC Proceedings Volumes*, vol. 38, no. 1, pp. 313–318, 2002.

[23] Y. Huo, L. Yang, T. Xu, and D. Sun. Design, Control, and Clinical Applications of Magnetic Actuation Systems: Challenges and Opportunities. *Advanced Intelligent Systems*, 2400403, 2024.

[24] F. White, *Viscous Fluid Flow*. New York: McGraw-Hill, 2006.

[25] C. Kravaris and J. C. Kantor, "Geometric methods for nonlinear process control. 1. background," *Industrial & Engineering Chemistry Research*, vol. 29, no. 12, pp. 2295–2310, 1990.

[26] A. Isidori, *Nonlinear control systems*. London: Springer, 1995.

[27] J.-M. Flaus, *La régulation industrielle : régulateurs PID, prédictifs et flous*. Paris: Hermes Science Publications, 1994.

Contribution of Individual Authors to the Creation of a Scientific Article (Ghostwriting Policy)
The authors equally contributed in the present research, at all stages from the formulation of the problem to the final findings and solution.

Sources of Funding for Research Presented in a Scientific Article or Scientific Article Itself
No funding was received for conducting this study.

Conflicts of Interest
The authors have no conflicts of interest to declare that are relevant to the content of this article.